Stanford Exploration Project, Report 115, May 22, 2004, pages 391–399

Migration methods for passive seismic data

Brad Artman, Deyan Draganov, Biondo Biondi, and Kees Wapenaar[1]

ABSTRACT

Passive seismic imaging is based on the fact that by cross-correlating the transmission responses of a medium, one can reconstruct its reflection response. Here, we show a method to directly migrate the transmission responses measured at the surface, based on the shot-profile migration. We also show that the results from direct migration of passive data and from migration of the simulated reflection response are identical. At the end, we also show comparisons between the behavior of the results from the migration process and the simulated reflection responses.

INTRODUCTION

In Wapenaar et al. (2004b), general relations are shown between the reflection and the transmission response of a 3-D inhomogeneous medium. The applications of these relations are in synthesis of transmission coda from reflection data, multiple elimination, seismic interferometry and acoustic daylight imaging. The relation used in the acoustic daylight imaging permits us to synthesize the reflection response of a medium by cross-correlating its transmission responses. Here, we show a method to directly migrate passive white-noise seismic data without the need to first perform the cross-correlations. We also compare the results of simulating the reflection response with the results from migration of the passive data.

DIRECT MIGRATION OF WHITE-NOISE DATA

To simulate the reflection response from the transmission responses measured at the surface in the presence of white-noise sources in the subsurface we can use the formula

$$R^{+}(\boldsymbol{x}_A,\boldsymbol{x}_B,\omega)+\left\{R^{+}(\boldsymbol{x}_A,\boldsymbol{x}_B,\omega)\right\}^{*}=\delta\left(\boldsymbol{x}_{H,A}-\boldsymbol{x}_{H,B}\right) - T^{-}_{obs}(\boldsymbol{x}_A,\omega)\left\{T^{-}_{obs}(\boldsymbol{x}_B,\omega)\right\}^{*}. \quad (1)$$

Above, $R^{+}(\boldsymbol{x}_A,\boldsymbol{x}_B,\omega)$ is the reflection response measured at point x_A at the surface ($\partial\mathcal{D}_0$) in the presence of an impulsive source at x_B, while $T^{-}_{obs}(\boldsymbol{x}_A,\omega)$ is the transmission response measured at the surface point x_A in the presence of noise sources in the subsurface. Downward

[1]**email:** brad@sep, D.S.Draganov@CiTG.TUDelft.NL, biondo@sep,C.P.A.Wapenaar@CiTG.TUDelft.NL

extrapolaton of $R^+(\boldsymbol{x}_A,\boldsymbol{x}_B,\omega)$ to common surface locations ξ_A,ξ_B at an arbitrarily greater depth is described by

$$R^+\left(\boldsymbol{\xi}_A,\boldsymbol{\xi}_B,\omega\right) = \int_{\partial\mathcal{D}_0}\int_{\partial\mathcal{D}_0}\left\{W^+\left(\boldsymbol{\xi}_A,\boldsymbol{x}_A,\omega\right)\right\}^* R^+(\boldsymbol{x}_A,\boldsymbol{x}_B,\omega) \left\{W^-\left(\boldsymbol{x}_B,\boldsymbol{\xi}_B,\omega\right)\right\}^* d\boldsymbol{x}_A d\boldsymbol{x}_B\,, \quad (2)$$

where $R^+\left(\boldsymbol{\xi}_A,\boldsymbol{\xi}_B,\omega\right)$ is the reflection response extrapolated from the surface to some subsurface level and $W^+\left(\boldsymbol{\xi}_A,\boldsymbol{x}_A,\omega\right)$ and $W^-\left(\boldsymbol{x}_B,\boldsymbol{\xi}_B,\omega\right)$ are forward-extrapolation operators. If we substitute equation (1) into equation (2) we obtain

$$R^+\left(\boldsymbol{\xi}_A,\boldsymbol{\xi}_B,\omega\right) = \int_{\partial\mathcal{D}_0}\left\{W^+\left(\boldsymbol{\xi}_A,\boldsymbol{x}_A,\omega\right)\right\}^* T^-_{obs}(\boldsymbol{x}_A,\omega)d\boldsymbol{x}_A \left\{\int_{\partial\mathcal{D}_0} W^+\left(\boldsymbol{\xi}_B,\boldsymbol{x}_B,\omega\right) r\,T^-_{obs}(\boldsymbol{x}_B,\omega)d\boldsymbol{x}_B\right\}^* + \text{anti-causal terms}\,. \quad (3)$$

In the above relation, we used the fact that the reflection coefficient of the free-surface is $r=-1$ and the reciprocity relation of the forward-extrapolation operator $W^-\left(\boldsymbol{x}_B,\boldsymbol{\xi}_B,\omega\right) = W^+\left(\boldsymbol{\xi}_B,\boldsymbol{x}_B,\omega\right)$. Equation (3) shows that by inverse-extrapolating the transmission response $T^-_{obs}(\boldsymbol{x}_A,\omega)$ at all $\boldsymbol{x}_A$ at the surface to a certain subsurface level, and forward-extrapolating the downward-reflected transmission response $rT^-_{obs}(\boldsymbol{x}_B,\omega)$ at all $\boldsymbol{x}_B$ to the same subsurface level, followed by cross-correlation of the resultant wave fields, we obtain the downward extrapolated reflection response. If we subsequently apply the imaging condition, we can image the subsurface at that level (Armtan et al., 2004)). If we compare this process with shot-profile migration (Claerbout, 1971) we can see that they are identical. This means that based on shot-profile migration we can directly migrate passive white-noise data without the need to first simulate the reflection shot gathers. As Figure 1 shows, we may thus use two paths for obtaining a migrated image from passive data. Following the first path, we first cross-correlate the transmission responses recorded at the surface to simulate reflection shot gathers, then we extrapolate the simulated shot gathers and apply the imaging condition (this process was also proposed by Schuster (2001) and named Interferometric Imaging). The other way is to directly migrate the passive data - first we extrapolate the transmission responses recorded at the surface to some subsurface level, then we cross-correlate them and apply the imaging condition. The left panel of Figure 2 shows a double syncline model used to generate transmission responses of white-noise sources in the subsurface. These transmissions were afterwards migrated using both migration methods described above. The results were identical (Figure 2).

SIMULATED REFLECTION VERSUS MIGRATION

In this section, we present some numerical results showing the behavior of the simulated reflection shot gathers and the migrated image when changing some source and receiver parameters. The migrations were performed with the exact velocity model. No multiple elimination

$$
\begin{array}{ccccc}
\boxed{T^-_{obs}(\boldsymbol{x}_A,\omega)} & \otimes & \boxed{\left\{T^-_{obs}(\boldsymbol{x}_B,\omega)\right\}^*} & = & \boxed{R^+(\boldsymbol{x}_A,\boldsymbol{x}_B,\omega)} \\
\Big\downarrow \left\{W^+\left(\boldsymbol{\xi}_A,\boldsymbol{x}_A,\omega\right)\right\}^* & & \Big\downarrow \left\{W^+\left(\boldsymbol{\xi}_B,\boldsymbol{x}_B,\omega\right)\right\}^* & & \Big\downarrow \left\{W^+\left(\boldsymbol{\xi}_A,\boldsymbol{x}_A,\omega\right)\right\}^*\left\{W^-\left(\boldsymbol{x}_B,\boldsymbol{\xi}_B,\omega\right)\right\}^* \\
\boxed{T^-_{obs}\left(\boldsymbol{\xi}_A,\omega\right)} & \otimes & \boxed{\left\{T^-_{obs}\left(\boldsymbol{\xi}_B,\omega\right)\right\}^*} & = & \boxed{R^+\left(\boldsymbol{\xi}_A,\boldsymbol{\xi}_B,\omega\right)}
\end{array}
$$

Figure 1: Two paths can be followed to obtain a migrated image from passive data.

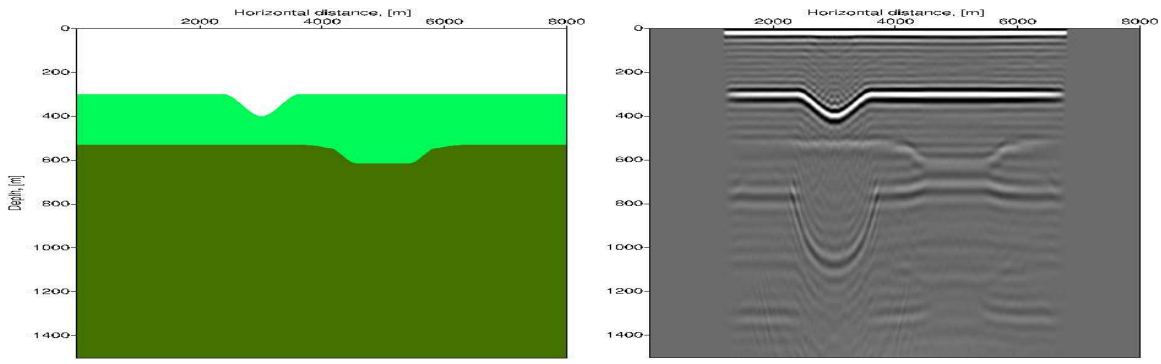

Figure 2: Left: Double syncline model with white-noise sources regularly distributed at depth level $x_3 = 800$ every 25m between $x_1 = 1200$ and $x_1 = 6800$ m. The transmission recordings were 66 minutes. Receivers at the surface are distributed between $x_1 = 1200$ and $x_1 = 6800$ m every 20 m. Right: The migrated image from the direct migration and the migration of the simulated reflection shot panels are identical. brad2-model [NR]

schemes were applied. The quality of the end result depends strongly on the number of the present subsurface sources. The left panels from Figures 3 through 6 show simulated reflection shot gathers for a decreasing number of subsurface noise sources with a simulated surface shot position at $x_1 = 4000$ m. The right panels from Figures 3 through 6 show the results from direct migration of the same noise recordings. The noise recordings were 6 minutes long. We see that the simulated reflection responses very quickly decrease in quality (compared with the directly modelled reflection response in Figure 11), while the migration process delivers much better results. Fewer source locations cause illumination problems in the migration result. The

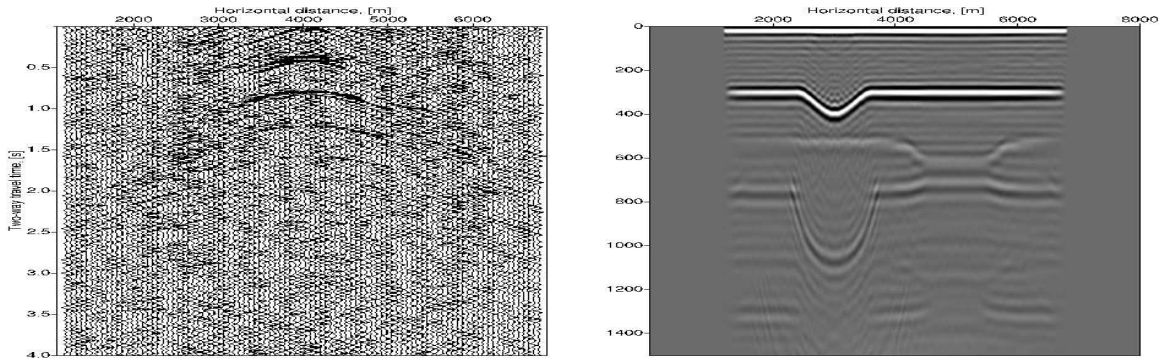

Figure 3: Left: Simulated reflection shot panel from 6 minutes long noise recordings with 113 regularly distributed subsurface sources with a simulated shot position at $x_1 = 4000$ m. Right: Result from direct migration of 6 minutes long noise recordings with 113 regularly distributed subsurface sources. brad2-dx_50m [NR]

left panels of Figures 7 through 10 show the change in quality of the simulated reflection shot gather (with simulated surface shot position at $x_1 = 4000$ m) when decreasing the recording time length of the receivers. The right panels of Figures 7 through 10 show the migrated image for the same noise recordings. We can see that while for short recording times the quality of the simulated reflection is strongly degraded, the result from migration is still good, only the signal-to-noise ratio has decreased. Note that multiple events that are hardly visible in the simulated reflection shot gathers at short recording times are still clearly present in the migrated image.

CONCLUSIONS

We showed the theoretical justification for directly migrating passive seismic noise recordings. This method is based on the shot-profile migration procedure, but is applied to transmission data. The results from the direct migration of passive data and from the migration of simulated reflection shot gathers are identical. Depending on the objective (to have intermidiate results or not) one or the other can be used. The numerical examples showed that while with decreasing number of subsurface noise sources and shorter noise recordings drastically reduced the quality of the simulated reflection response, the migration process still delivers good results.

Lastly, correlation of each trace with every other trace produces N shot gathers each with N traces from a survey with N receivers. If correlations are performed in the frequency domain, N^2 traces must be inverse Fourier transformed after multiplication to produce the shot-gathers. This requirement is especially onerous when the record length is at least minutes long. Then, another Fourier transform of N^2 traces, though now only seconds long, must be performed to make a $f-k$ based migration. Finally, the increased I/O associated with migrating N shots in a shot-profile migration are substantial compared with the single shot, even with many more frequencies, for direct migration utilizing an algorithm parallelized over frequency.

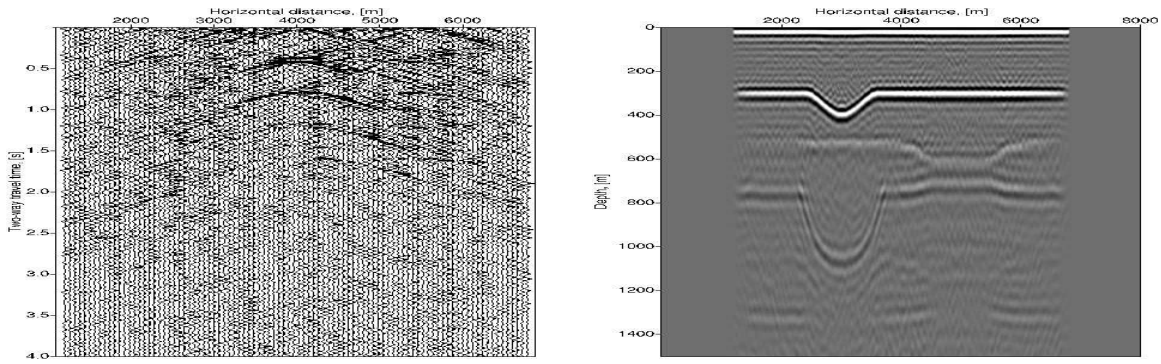

Figure 4: Left: Simulated reflection shot panel from 6 minutes long noise recordings with 57 regularly distributed subsurface sources with a simulated shot position at $x_1 = 4000$ m. Right: Result from direct migration of 6 minutes long noise recordings with 57 regularly distributed subsurface sources. brad2-dx_100m [NR]

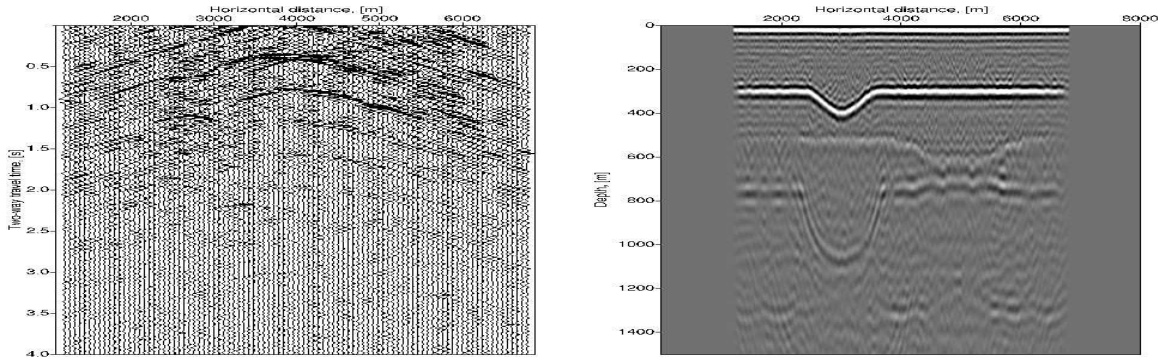

Figure 5: Left: Simulated reflection shot panel from 6 minutes long noise recordings with 11 regularly distributed subsurface sources with a simulated shot position at $x_1 = 4000$ m. Right: Result from direct migration of 6 minutes long noise recordings with 11 regularly distributed subsurface sources. brad2-dx_500m [NR]

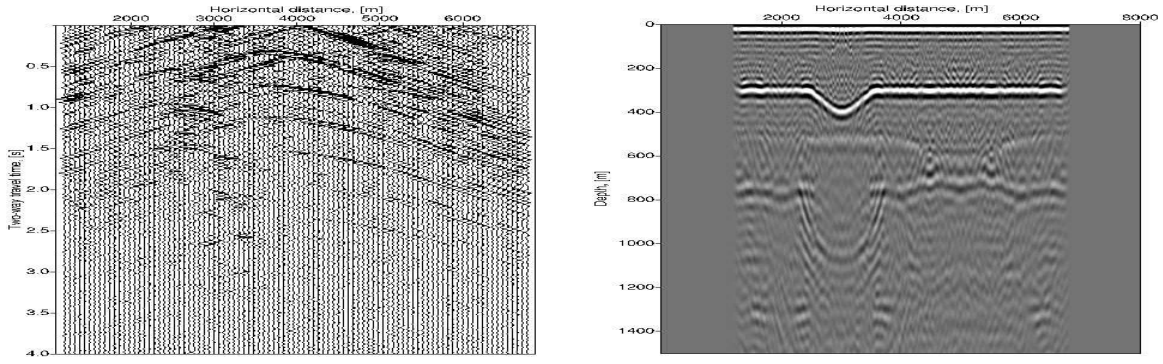

Figure 6: Left: Simulated reflection shot panel from 6 minutes long noise recordings with 6 regularly distributed subsurface sources with a simulated shot position at $x_1 = 4000$ m. (b) Result from direct migration of 6 minutes long noise recordings with 6 regularly distributed subsurface sources. brad2-dx_1000m [NR]

ACKNOWLEDGMENTS

This research is performed as part of research projects financed by the Dutch Science Foundation STW (number DTN4915), the Dutch Research Centre for Integrated Solid Earth Sciences - ISES and the Stanford Exploration Project.

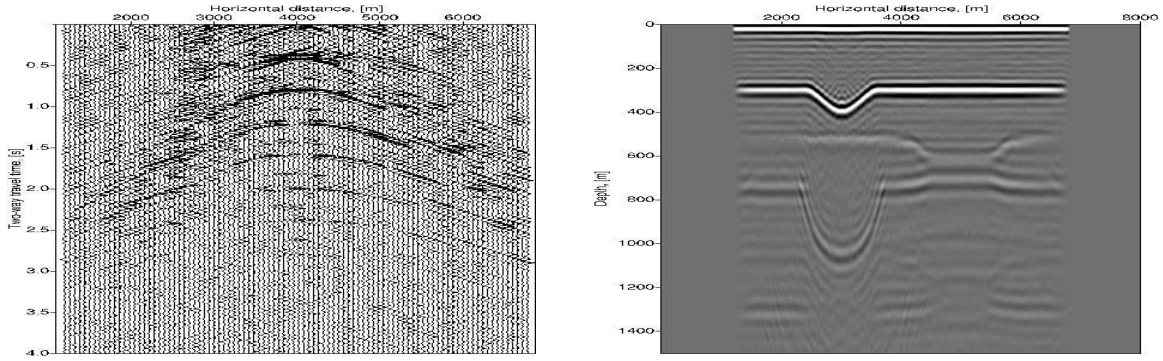

Figure 7: Left: Simulated reflection shot panel from 33 minutes long noise recordings with a simulated shot position at $x_1 = 4000$ m. Right: Result from direct migration of 33 minutes long noise recordings. brad2-t_33m [NR]

REFERENCES

Armtan, B., Draganov, D., Wapenaar, C., and Biondi, B., 2004, Direct migration of passive seismic data: Europ. Assoc. Geosc. Eng., Extended abstracts, P075.

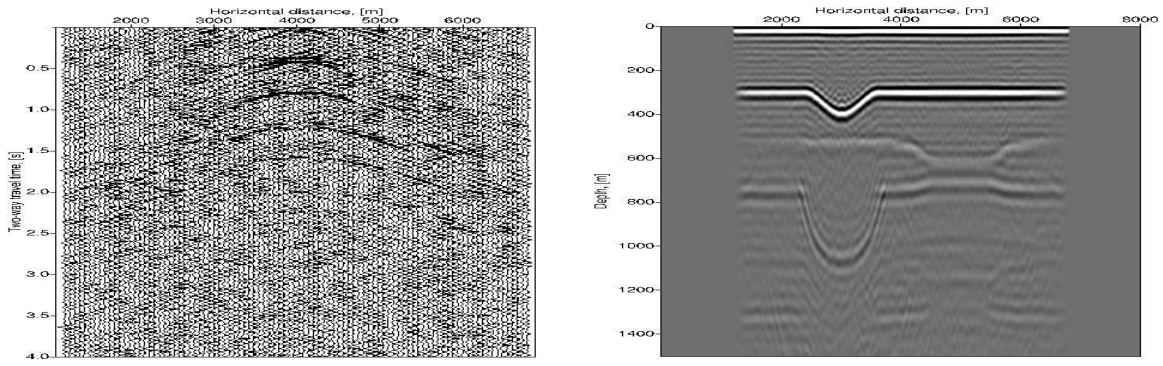

Figure 8: Left: Simulated reflection shot panel from 6 minutes long noise recordings with a simulated shot position at $x_1 = 4000$ m. Right: Result from direct migration of 6 minutes long noise recordings. brad2-t_6m [NR]

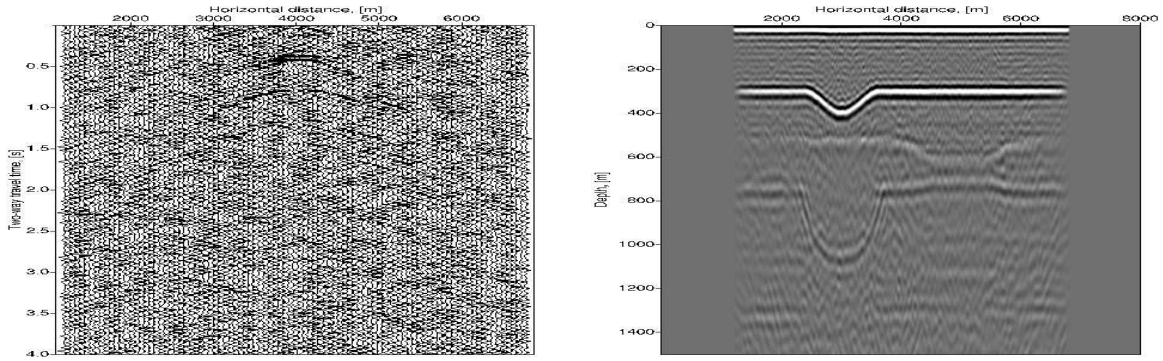

Figure 9: Left: Simulated reflection shot panel from 1 minute long noise recordings with a simulated shot position at $x_1 = 4000$ m. Right: Result from direct migration of 1 minute long noise recordings. brad2-t_1m [NR]

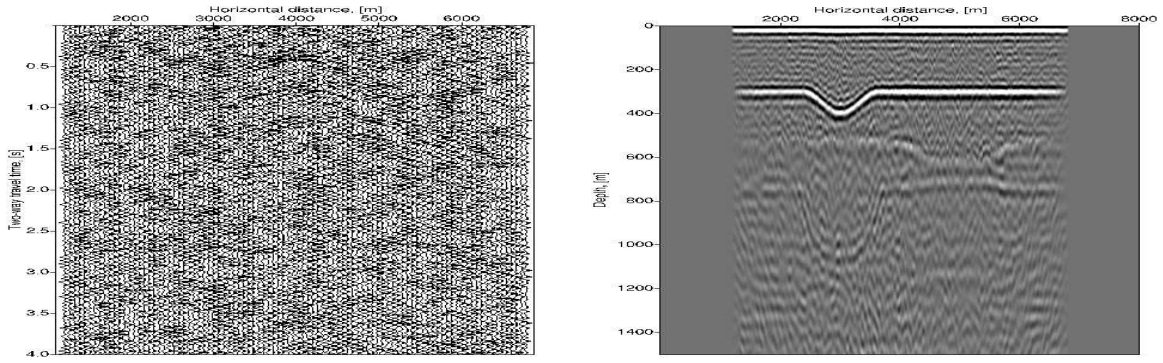

Figure 10: Left: Simulated reflection shot panel from 20 seconds long noise recordings with a simulated shot position at $x_1 = 4000$ m. Right: Result from direct migration of 20 seconds long noise recordings. brad2-t_20s [NR]

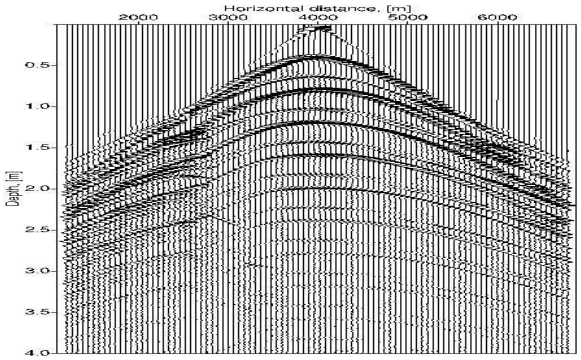

Figure 11: Directly modelled reflection response for the double syncline model from figure 2 (a) with a shot at $x = (4000, 0)$ m. brad2-refl [NR]

Claerbout, J. F., 1971, Toward a unified theory of reflector mapping: Geophysics, **36**, no. 03, 467–481.

Schuster, G., 2001, Theory of Daylight/Interferometric Imaging - Tutorial: Eur. Assn. Geosci. Eng., 63rd Mtg., Session: A–32.

Wapenaar, C., Thorbecke, J., and Draganov, D., 2004b, Relations between reflection and transmission responses of 3-d inhomogeneous media: Geophys. J. Int., **156**, 179–194.